Applied Surface Science 597 (2022) 153676

Contents lists available at ScienceDirect

Applied Surface Science

journal homepage: www.elsevier.com/locate/apsusc

Full Length Article

Micro-structured and self-assembled patterns in PLA-cast films as a function of CTAB content, magnesium and substratum hydrophobicity

Amparo M. Gallardo-Moreno [b,a,c,1], Verónica Luque-Agudo [a,b,c,1], M. Luisa González-Martín [a,b,c,*], Margarita Hierro-Oliva [a,b,c]

[a] Universidad de Extremadura, Facultad de Ciencias, Departamento de Física Aplicada, Badajoz, Spain
[b] Centro de Investigación Biomédica en Red: Bioingeniería, Biomateriales y Nanomedicina (CIBER-BBN), Badajoz, Spain
[c] Instituto Universitario de Investigación Biosanitaria de Extremadura (INUBE), Badajoz, Spain

ARTICLE INFO

Keywords:
Micro-topography
Atomic force microscopy
Polylactic acid
Cetyltrimethylammonium bromide
Magnesium
Degradation

ABSTRACT

The fabrication of biomaterials with structured surfaces for medical purposes is a topic of great interest. Producing topographies with certain characteristics can benefit tissue formation and/or reduce the probability of developing an infection due to the hindrance shown by certain micro-structures to microbial adhesion.

This work presents a new, economically attractive way to fabricate micro-structured patterns on the surface of one of the currently most interesting bioabsorbable polymeric materials, polylactic acid (PLA). Formation of homogeneously distributed holes is presented as a function of three factors: the concentration of cetyltrimethylammonium bromide (CTAB), the presence or not of the dispersant magnesium, and the hydrophobicity of the support used in the PLA-film fabrication, silicone or glass. The size of the holes increases with the CTAB concentration: from 1 to 5 μm on silicone and 2 to 20 μm on glass. Magnesium particles make CTAB to disperse better inside the PLA matrix, provoking the irregular holes observed on glass become regular with sizes between 0.5 and 2 μm. The topographies obtained on silicone are highly stable over time, while on glass they degrade after 28 days. Consequently, it is possible to design a wide spectrum of micro-structured topographies, covering both antimicrobial and tissue integration targets.

1. Introduction

Nowadays, the concept of "green plastic" is very important in the manufacture of polymers in any sector [1], since many of the polymers produced are based on petroleum, a non-renewable raw material. In this context, polylactic acid (PLA) is a highly interesting polymer due to its recognized biodegradability, non-toxicity and biocompatibility, properties which make it extremely attractive from an industrial [2] and biomedical [3] point of view.

Production of PLA films by solvent casting is a widely used and easy to apply technique [4–8]. It consists of dissolving the polymer in a suitable solvent, casting it on a substrate and allowing it to dry. In this way, both the solvent and the substrate used for deposition can influence the surface properties of the films and can be selected in accordance with the surface properties desired. Paragkumar et al. [9] and Sato et al. [5], in independent studies, showed that the solvent of choice induces conformational changes in the polymer structure, and Byun et al. [4] attributed these changes to alterations in crystallinity. For their part, Fukuoka et al. [10] found changes in hydrophobicity depending on the material on which the solution was cast, and our own studies have recently reported that interaction free energy of two PLA surfaces immersed in water is also highly influenced by the support surface [11].

Another way of changing the properties of casting-solvent PLA films is by introducing dopants into the polymeric matrix [12–15] and there are numerous possibilities to include these dopants into the PLA matrix. A possibility related to improving the mechanical properties of PLA is the inclusion of metallic particles. In this sense, copper, bronze and silver have been used as micro-fillers of PLA nanocomposites, due to their additional antibacterial properties [16]. PLA functional fillers are also zinc oxide and silver-copper alloy nanoparticles [17] and silicon-hydroxyapatite or magnesium-hydroxyapatite for promoting osteogenic properties [18]. One of the most used metallic particles is magnesium [19,20]. The incorporation of magnesium particles into PLA matrices is always associated to the manufacture of biodegradable

* Corresponding author at: Universidad de Extremadura, Facultad de Ciencias, Departamento de Física Aplicada, Badajoz, Spain.
E-mail address: mlglez@unex.es (M.L. González-Martín).
[1] These authors contributed equally to this work.

https://doi.org/10.1016/j.apsusc.2022.153676
Received 8 February 2022; Received in revised form 4 May 2022; Accepted 12 May 2022
Available online 16 May 2022

materials, mainly in those cases where a change in the mechanical properties of PLA is sought for use in temporary bone repairs. Adding magnesium to PLA brings the Young's modulus of the composite closer to that of bone and modulates the polymer degradation rate of PLA that in most of the biomedical applications is consider too low. Moreover, these mechanical changes have been accompanied by beneficial bactericidal effects associated to the dissolution of magnesium particles, which provokes microenvironments of high pH and hydrogen concentration, favouring bacterial damage. Other types of dopants, e.g. surfactants such as cetyltrimethylammonium bromide (CTAB) can be used to improve the wettability of PLA [10,21–23]. Moreover, CTAB is also a surface modifier, so it is used to achieve a homogeneous distribution of magnesium particles in the polymeric matrix [20,23]. This better distribution is mainly due to attractive electrical interactions between the magnesium particles and the CTAB molecules, a fact that even affects the distribution of the components in the matrix in an internal layer-like model of the film.

In order to assess how the PLA biomaterial may behave in an *in vivo* setting, studies have focused on evaluating its response to bacterial and cell adhesion and proliferation [7,24–27]. In this line of studies, the surface is crucial because in addition to the active components that the PLA matrix can support to prevent infection and promote cell integration [7,24,28,29], the topography of the surface can alter the adhesive behaviour of these cells, whose size is within the micrometric scale.

In this regard, there are numerous studies that relate the topography of a surface to both microbial and cellular adhesion processes [30–34]. The size, shape and distribution of topographical structures play an important role in the attachment of bacteria and cells to the surface of biomaterials.

Focusing on the antimicrobial properties of biosurfaces, several studies have shown that certain structures, ranging from random structures to ordered arrays, on the surface of biomaterials do not promote bacterial adhesion [30,31]. It is a common observation that when the pitch size of the structure is smaller than the size of the bacteria, fewer bacteria adhere to surfaces [35]. In addition, previous studies by our research group demonstrated that surfaces with spatially organised micro-topographical patterns lead to a significant reduction in bacterial adhesion relative to smooth control samples [36]. In the same vein, Xiang Ge and co-workers demonstrated that sub-micrometre-scale patterns effectively inhibit bacterial adhesion, growth and colonisation by physically preventing bacterial cell–cell interactions [37]. Studies by Audrey Allion et al. showed that bacterial adhesion was reduced on micro-topographies of the stainless-steel surface generated by a unidirectional polish finish relative to the smooth surface [38]. More recent studies by A.-K. Meinshausen et al. show that surface structuring can decrease the amount of adherent bacteria on implants made of titanium and polyester polyethylene terephthalate (PET) [39]. In the review by Abinash Tripathy et al. a complete overview of natural and bio-inspired nanostructured surfaces, both with random structures and ordered arrays, with bactericidal power is provided [40].

In the particular case of biodegradable materials, the topography of a surface can be modified as a result of degradation in physiological media [41–43], especially if the materials are loaded with substances that are very active or reactive in aqueous media, as is the case of magnesium [7,44] and surfactants [23,45]. Particularly, in contact with water, magnesium forms a hydroxide, soluble up to pH = 10.5, and precipitates above this pH value. However, in physiological buffers containing chloride anions, as in phosphate buffer saline (PBS), both metallic magnesium and its hydroxide react with the chloride, resulting in magnesium chloride, which is much more soluble in water and, in turn, increases the solubility of the magnesium metal, increasing the Mg^{2+} cation concentration and pH [46]. This degradation of the biomaterial can progressively release the active components into the environment and significantly alter the topography that the material can expose to the surrounding media and, in consequence, its response against cell and bacterial adhesion.

Within this scenario, the main objective of this work is to analyse topographically the micro-structures formed "spontaneously" on the surface of PLA films when different concentrations of the surfactant CTAB are added and to evaluate how these structures are modified when magnesium is added to the polymeric matrix. The study includes an analysis of the stability of the structures as a function of time, by immersing the films in PBS for 7 and 28 days. The procedure followed and the diversity of structures observed will serve to propose a new versatile method for the creation of structured patterns on biopolymers.

2. Materials and methods

2.1. Films preparation

Glass disks were cleaned with chromic acid, rinsed with deionized water, and dried at 37 °C. Silicone disks were cleaned with absolute ethanol and dried with a flow of N_2. All disks were stored in a desiccator until use.

Films were prepared as described in our previous work [23]. In brief, polylactic acid (PLA) particles (PLA2003D, with D-isomer content of 4.25%, purchased from NatureWorks LLC, Blair, NE, USA) were dissolved in chloroform (Sigma-Aldrich, Merck, Darmstadt, Germany) (5% w/v) using a rotator stirrer (JP Selecta, Barcelona, Spain). Then, different amounts of cetyltrimethylammonium bromide (CTAB, Sigma-Aldrich, Merck, Darmstadt, Germany) (0, 1, 5 and 10% w/w with respect to PLA) were added and the solutions were homogenised by stirring. To prepare the batch of magnesium-containing solutions, magnesium particles (≤50 μm, Nitroparis, Castellón, Spain) were added and stirred to achieve a final concentration of 3% w/w relative to PLA.

Once the solutions were prepared, 1 or 2 mL of each mixture was cast on silicone and glass disks, respectively, and left to dry at room temperature for 24 h. Then, films were dried in an oven at 70 °C for 24 h, in order to remove completely any remaining solvent. After drying, the films were peeled off from the host surfaces. Films were stored in a desiccator until use. Characterisation of the films by the techniques described in the following sections was carried out before and/or after gently rinsing the film surface with a volume of 1 mL of Milli-Q water for 5 min. Rinsing was followed by air-drying prior to characterisation.

2.2. In vitro degradation

Films were immersed in 30 mL of phosphate buffer saline (PBS) at 37 °C for 7 and 28 days. After degradation, films were dried with a flow of N_2 and stored in a desiccator until use.

Since the number of samples is high, to better follow the results, the notation used is the following: X-Y/Z_D, X being the substrate used (S or G), Y the amount of magnesium added (0 or 3% w/w), Z the amount of surfactant added (0, 1, 5 or 10% w/w) and D the number of days of degradation (7 or 28).

2.3. Surface structure characterization

Surface morphology of PLA films was evaluated using an atomic force microscope (AFM) (Agilent AFM 5500, Agilent Technologies, California, CA, USA) operating at room temperature and in contact mode. Rectangular cantilevers (FMV-PT, Bruker, USA) were used with a nominal spring constant of 75 kHz and a force constant of 3 N/m. Images were taken at different scanning lengths from 50 × 50 μm^2 to 5 × 5 μm^2 depending on the size of the features to be analysed. In each scanning area, topographical, deflection and friction images were acquired. Three different films were studied of each condition (triplicate) and 5 different regions on each film surface were scanned. Since roughness is a scale-dependent function, all the comparisons were made with the average roughness (Sa) obtained from 50 × 50 μm^2 images. Any features observed in the images were characterized from line profiles, and their width and depth measured. Results are given as average values and

standard deviations.

2.4. Surface chemical composition

Time of flight secondary ion mass spectrometry (ToF-SIMS) analyses of samples were performed with a Tof-SIMS^5 (ION TOF, Münster, Germany) using a Bi_3^{2+} as primary gun, operating at 25 keV. The total ion dose used to acquire each spectrum was above 10^{12} ions/cm^2. Negative spectra were recorded, and a pulsed low energy electron flood gun was used for charge neutralization.

2.5. Hydrophobicity

Water contact angles on films were used as a measure of their

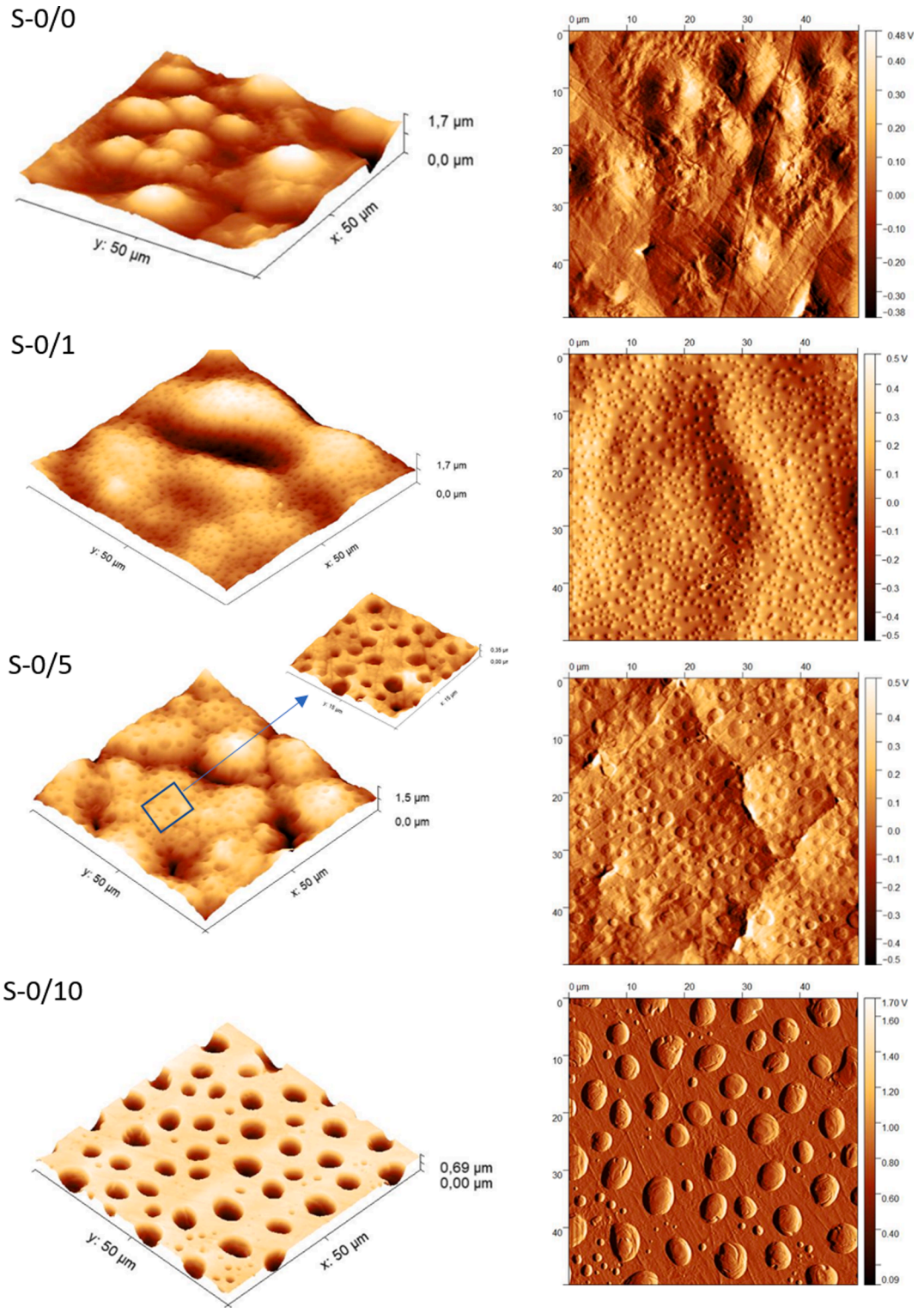

Fig. 1. AFM images of films cast on silicone, without magnesium and with different concentrations of CTAB. Left and right images are topographical and deflection images, respectively.

hydrophobicity. Films were placed on the stage of a Drop Shape Analyzer-DSA100E system (Krüss, Hamburg, Germany) and drops of 5 μL of Milli-Q water were placed on their surface. Sessile drops were analysed by ADVANCE for Drop Shape Analyzer (Version 1.12–01). At least two drops were measured in the central part of each film and three different films were studied of each condition.

2.6. Surface tension of degradation media: CTAB release quantification

Drop Shape Analyzer-DSA100E system (Krüss, Hamburg, Germany) was used for pen-dant drop tensiometry to measure the surface tension of the PBS degradation media after immersing the films for 7 and 28 days. The volume of the drops ranged between 20 and 30 μL, and 5 measurements were made for each liquid analysed.

The changes in the surface tension of the PBS after film degradation were used to estimate the concentration of CTAB released. For this purpose, the surface tensions of a series of solutions with concentrations ranging from 0 to 0.16 mg/mL of CTAB (minimum and maximum CTAB concentrations expected) were measured, and the data were fitted to an exponential-like equation. The CTAB concentrations of the immersion media for each film and time were calculated from this equation.

3. Results and discussion

3.1. Silicone-cast films

Films prepared by solvent-casting permit working with both sides: the one in contact with the substrate and the one exposed to the air. Some works discuss the surface properties of the films depending on the side chosen [10] and in some cases the research is carried out on one specific side [11]. In our study we fixed the side in contact with the substrate (bottom side) to allow a better comparison between samples.

3.1.1. Topography of non-degraded films

Fig. 1 shows some representative images of the topography of films cast on silicone without magnesium, with the different amounts of CTAB. Left and right images are topographical and deflection images, respectively. In the case of S-0/0, the film surface replicated the topography of the silicone substrate, where some scratches and indentations appeared, revealing areas with a different polymer accumulation. This caused the images to have two different roughness values: Sa = 240 ± 30 nm, (in areas with higher accumulations of PLA, this is the case shown in Fig. 1) and Sa = 50 ± 20 nm (very flat and uniform PLA finish, see Fig. S1 in the Supporting Information). The 1 mL volume of water deposited on the film surface to gently clean the surface of these films (without CTAB) did not alter the topography or the roughness (images of films prior to cleaning not shown).

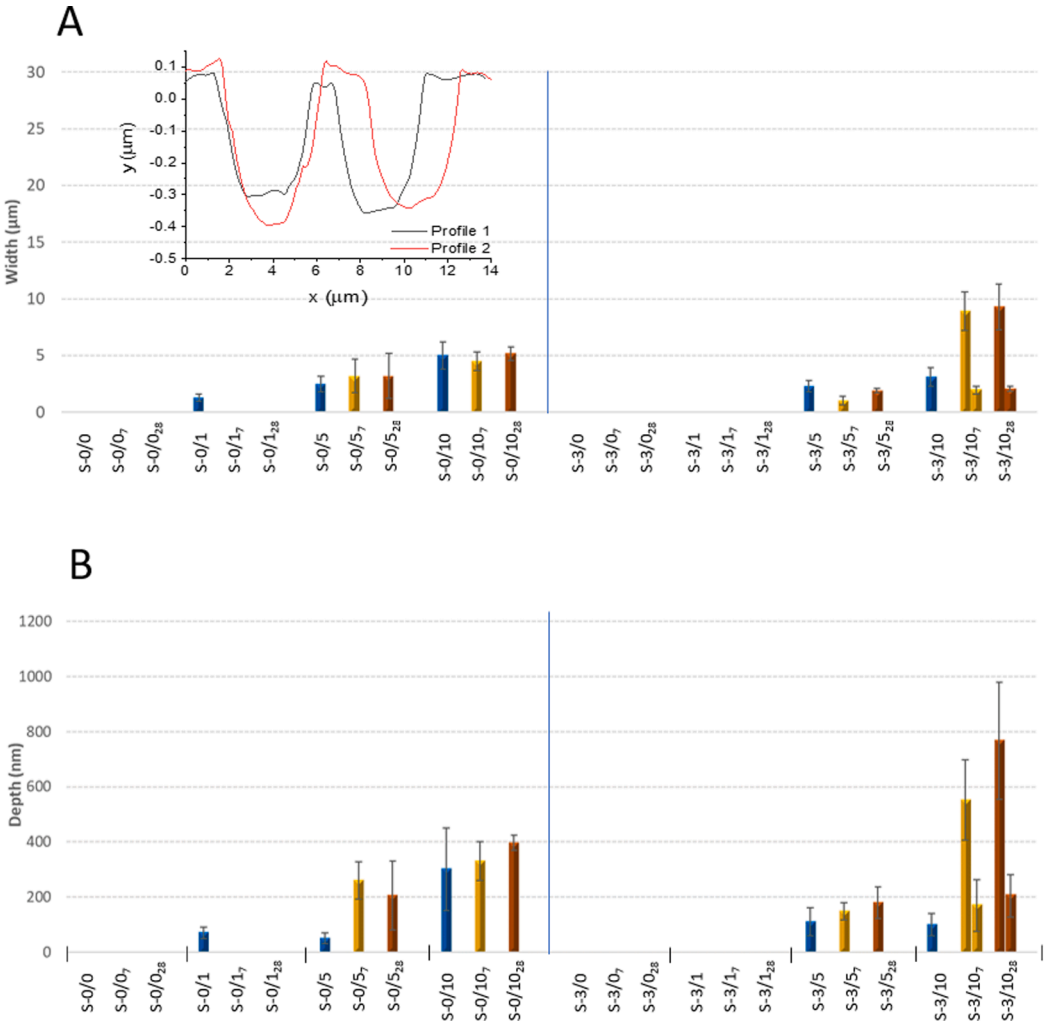

Fig. 2. Quantification of the features (holes) observed on films deposited on silicone through their width (A) and depth (B). Two bars for the same sample indicate the presence of two completely different hole populations.

As CTAB was added (S-0/1, S-0/5, S-0/10), hole-like structures appeared on the surface of the films after rinsing, whose sizes increased with the amount of surfactant. Fig. 2 statistically quantifies the features of each sample: Fig. 2A-width and Fig. 2B-depth. The inlet of Fig. 2A is only an example of two line profiles (two holes each), used to carry out the measurements. It should be noted that in any case the roughness of the samples is dominated by the roughness of the polymer and therefore it is difficult to find significant differences in this parameter in relation to the control (S-0/0). Differences were found in the size of the structures, the width changing from 1.3 ± 0.3 μm in the case of S-0/1 to 2.5 ± 0.7 μm for S-0/5 and 5.0 ± 1.2 μm in the case of S-0/10. The depth was significantly increased with the highest amount of surfactant: from about 60 nm to 300 nm (average).

The formation of holes in the surface of the films must be related with the distribution of surfactant inside the polymeric matrix. During the drying process, the excess of surfactant in the polymeric matrix is segregated to the surface and it accumulates in specific very well-distributed areas of the surfaces. During the gentle washing of the surface, the surfactant dissolves rapidly in the water, leaving its "footprint" on the surface. The size of these areas depends on the amount secreted which, in turn, is a function of the surfactant concentration in the film.

To demonstrate this hypothesis, freshly prepared films were visualized without rinsing and after gentle washing. As an example, Fig. 3 shows the appearance of an S-0/10 film before rinsing (Fig. 3A) and after gentle cleaning (Fig. 3B). In the case of the films before rinsing, there is no evidence of holes on the surface in the topographic images; the surface appears relatively flat, with circular-like contours slightly visible in some areas (see the arrows). However, the friction images offer useful information: these images can give us details of compositional changes as long as the modifications in colour are not directly associated to topographic features, and this is what happens experimentally: circular-like structures with different compositions from the rest of the materials are appreciated, coinciding in diameter with the width of the hollows of the sample S-0/10. When the surface is slightly washed (Fig. 3B) these "filled" cavities are rapidly emptied, giving rise to the patterns already observed in Fig. 1.

The distribution of surfactants within polymer films is of great interest in the case of films prepared from aqueous colloidal dispersions, in which surfactants are primarily required to ensure the stability of the colloidal particles. Within this scenario, the idea of segregation-exclusion of the surfactant is in agreement with the research of other authors. The previous work of Du Chesne et al. showed that, using energy filtering transmission electron microscopy, it was possible to detect domains of emulsifiers (surfactants) on the surface and in the bulk of thin latex films prepared from solvent-casting at temperatures higher than the so-called minimum film-forming temperature [47]. An excess of surfactant at the film-air interface is also deduced by Mallegol et al. in their work with waterborne acrylic pressure-sensitive adhesives, causing latex particles not to aggregate [48]. The migration of surfactant to interfaces is driven by its tendency to lower its interfacial free energy in the water solution, provoking a decrease in the interfacial energy at the polymer/air and polymer/substrate interfaces. An excess concentration of surfactants can develop at and near interfaces during the drying stage, and segregation and exudation can also occur depending on the film formation or storage temperature. However, although in that work they make an interesting topographical study of the films by AFM, they do not clearly observe the surfactant exclusion zones on the surface. The work of Monteiro et al. does describe the formation of holes in latexes of block copolymers, after removing the surfactant by rinsing, and associates this effect to the slow coalescence of the particles during drying [49].

In any case, the studies carried out on these structures have been associated with the particular distribution of particles in latex-like lattices, and they have not been observed so far in polymeric matrices such as PLA as a function of magnesium content and substrata hydrophobicity.

Although, as mentioned, we focussed on the bottom side of the films (in contact with the substrate), some extra experiments were also made on the top part (in contact with air) to support the hypothesis of

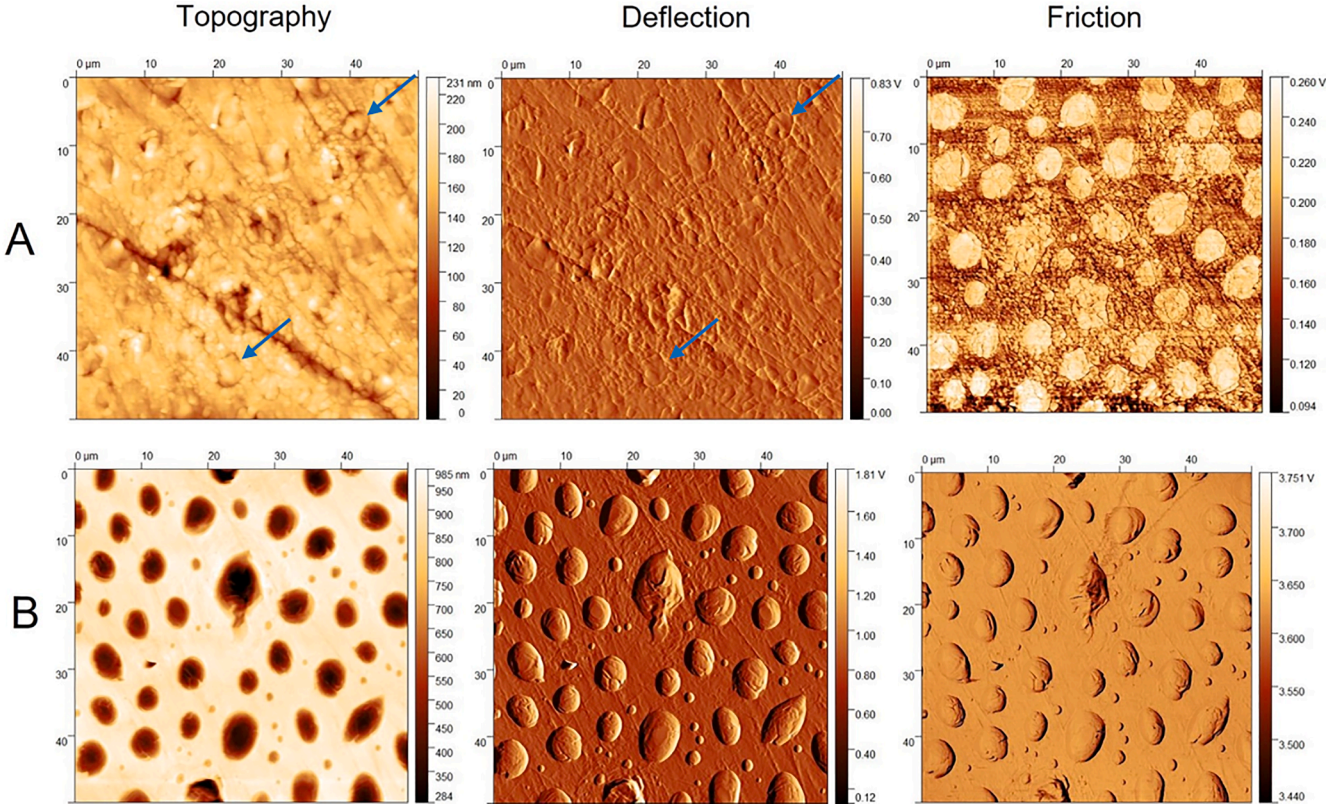

Fig. 3. Topographic, deflection and friction AFM images of S-0/10 freshly prepared films, without rinsing (A) and after washing (B).

surfactant accumulation and exclusion areas. This information is included in the supporting information (Fig. S2) and the results agree with the previous work of Zhang and Severtson, who reported that the faster drying on the top surface than on the bottom surface caused a more abrupt and less organized accumulation of surfactant than on the bottom side [21]. Images from Fig. S2 show the formation of irregular holes in the S-0/10 (top) sample, much higher than in the case of S-0/10 (bottom). For the sake of comparison, the features width from the top reached values of up to 20 μm, while from bottom they were not, in general, higher than 7 μm.

When magnesium particles were added to PLA films containing varying amounts of CTAB, the hole-like structures described above in Fig. 1 did not alter significantly and the sizes were similar to those obtained for non-containing magnesium samples, as can be seen in Fig. 2. It is worth noting that in the case of S-3/1 no area of the film surface was found to show the small holes observed in S-0/1. Magnesium probably helps to homogenize the CTAB content, as the surfactant adsorbs on the surface of the magnesium particles. This reflection is in line with the work of other authors who used CTAB to better disperse these particles in the PLA polymeric matrix, when working with higher magnesium concentrations than those used in this research [20].

3.1.2. Topography of degraded films

The next step for characterizing these structures on the surface of the films was to check how stable they are against degradation of the material, taking into account that this polymer can be used for biomedical purposes.

In the cases without magnesium (Fig. 2, left) the immersion in physiological buffer at 37 °C for 7 and 28 days did not seem to affect significantly the holes width for S-0/5 and S-0/10; in the case of S-0/1 the small holes disappeared, probably because of the deposition of salts coming from the PBS during degradation. In the case of depth, only for S-0/5 was the hole depth increased from 50 nm to about 230 nm (in average) with degradation, which could be associated to a more efficient cleaning of the hole by the surfactant.

In the case of films containing magnesium particles, degradation significatively affected films with the highest amount of CTAB (Fig. 2 right), regardless of the degradation time. Fig. 4 presents some example images of S-3/5_7 and S-3/10_{28}. In S-3/10_{28} some structures became wider and deeper than in the case of S-3/10 with a more irregular conformation; their quantification in Fig. 2 shows that changes were close to 200 % for width and to 450% and 670% for depth in S-3/10_7 and S-3/10_{28}, respectively. In these cases, there were also a number of small holes on the images with sizes close to the sample without degradation These hole populations are also plotted in Fig. 2 (including a second column in the figure for that sample).

The absence of topographical changes between 1 week and 4 weeks of degradation must be related to a certain balance between surfactant release (increase in the hole dimensions) and an accumulation of salts from the PBS in the holes (decrease in the hole dimensions). This idea is based on the studies carried out on the quantification of surfactant in the degradation medium with the degradation time.

Fig. 5 presents the estimation of the surfactant concentration in the degradation media. For films without and with magnesium, the concentration of CTAB in the degradation medium increased with the surfactant content. Similar values of CTAB were found in samples with 1% CTAB and 5% CTAB at both degradation times and only in the case of 10% CTAB was the released surfactant amount significantly higher at 28 days than at 7 days. Since we found no differences in feature sizes of S-0/10_7 and S-0/10_{28} or of S-3/10_7 and S-3/10_{28}, it is very likely that the release of CTAB occurred simultaneously with the deposition of salts during degradation. Probably the presence in the case of S-3/10_7 and S-3/10_{28} of small holes is due to the release of CTAB from the whole polymer matrix, a fact that is also supported by the fact that magnesium helps to disperse the surfactant within the polymer. It is very likely that the surfactant located on the surface of the magnesium particles (or near) forms small aggregates when these particles are degraded with time: the dissolution of magnesium particles and its transformation into Mg^{2+} is associated with a significant local increase in pH which may favour the agglutination of the CTAB molecules due to the suppression

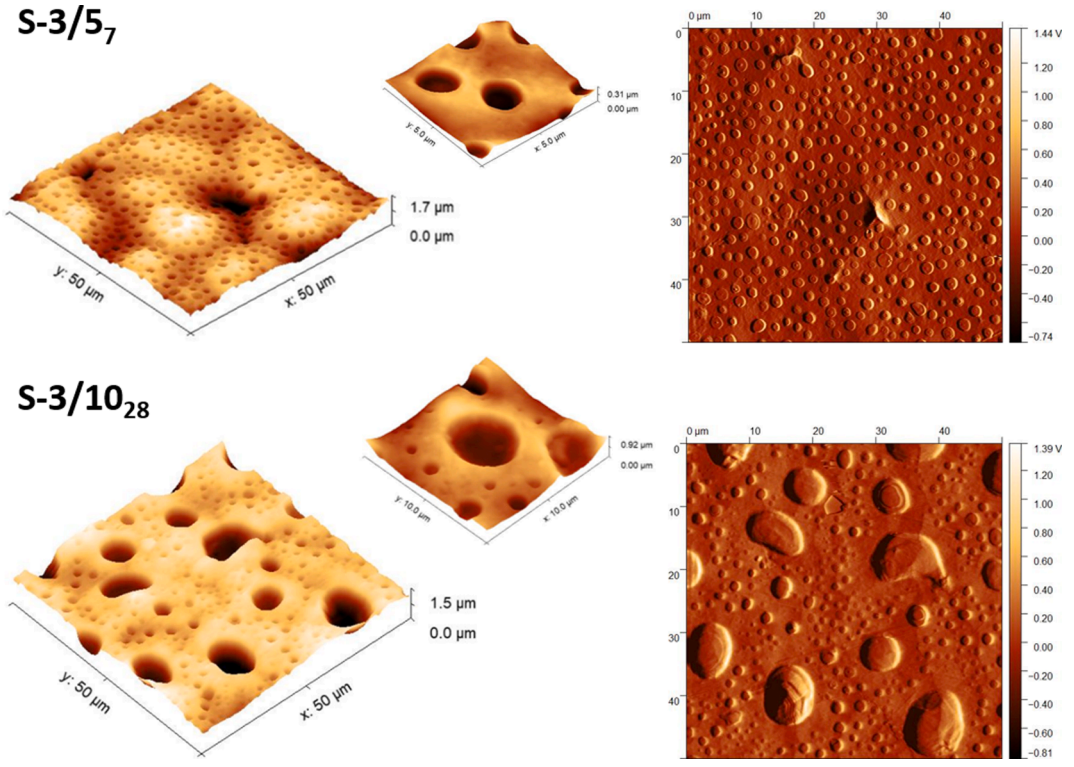

Fig. 4. Some representative AFM images of films deposited on silicone with magnesium and with CTAB after degradation. Left and right images are topographical and deflection images, respectively.

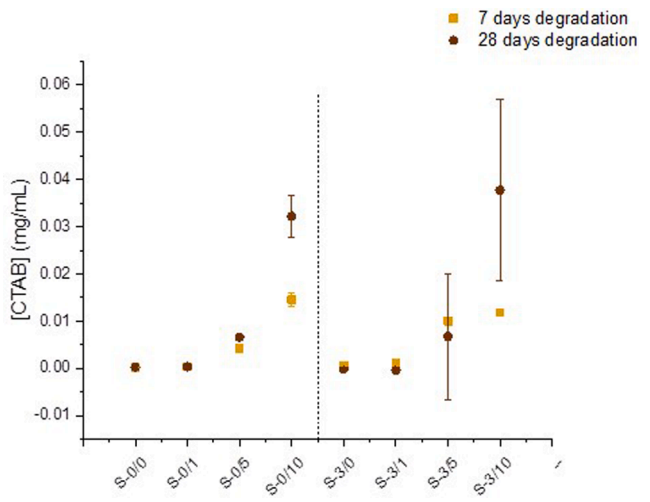

Fig. 5. Estimation of the surfactant concentration in the degradation media of films cast on silicone.

of the electrical repulsions between the cationic parts of the CTAB [46]. This idea is in line with the adsorption model proposed by Ferrández-Montero et al, where positive CTAB chains were adsorbed on the negative-charged magnesium particles [20]. The release into the medium of these aggregates would leave small footprints in the polymer that would be associated with the small holes observed. This process may be enhanced by degradation time and perhaps for this reason also the amount of CTAB at 28 days of the samples with magnesium reached the highest values.

Estimation of CTAB release to the degradation media was also combined with information of the chemical surface analysis of the films provided by the ToF-SIMS surface mass spectra, the bromide ion (Br^-) being chosen as a representative fragment of the CTAB and the $C_4H_7O_2^-$ fragment as a representative for PLA. Focussing on the cases with significant changes in CTAB concentration, Fig. 6A indicates that, within experimental error, Br^- is poorly detected on the surface of films from 7 days of degradation i.e. the most external film surface is "without" CTAB. For this reason, the differences in the surfactant concentration in the suspending liquid between 7 days and 28 days should come from the surfactant diffusion from the bulk PLA matrix. Considering that the amount of CTAB loaded to the film represents 100% of the amount that can be found in the degradation medium, the average amount of CTAB found in the degradation medium for S-0/10_7, S-3/10_7, S-0/10_{28} and S-3/10_{28} was 5.5%, 4.2%, 22% and 47%, respectively, indicating that at 28 days the release of CTAB with magnesium is twice as much as without magnesium.

3.2. Glass-cast films

3.2.1. Topography of non-degraded films

Fig. 7 presents some representative images of the films without magnesium, G-0/0, G-0/1, G-0/5 and G-0/10. The topography of control films deposited on glass, G-0/0, was very uniform and smooth, replicating the glass surface, without areas of higher or lower polymer accumulation, as happened with silicone, and their roughness was low, Sa = 4 ± 1 nm. When CTAB was added to the film this roughness increased with the CTAB concentration: 12 ± 5 nm; 70 ± 12 nm; 150 ± 15 nm for G-0/1, G-0/5 and G-0/10, respectively. The addition of CTAB caused structures to appear on the surface of the film. In the case of G-0/1 such patterns were more clearly visible than on silicone and larger. By adding more CTAB, these structures became larger and more irregular, especially in the case of G-0/10. Fig. 8 quantifies, on average, the size (width and depth): in the case of G-0/10, two groups were made, relating to larger and smaller structures (Fig. 7). The width of the holes doubled from G-0/1 to G-0/5 (2.0 ± 0.5 μm to 4.1 ± 1.5 μm) and these structures became extremely wide for the G-0/10 condition (20 ± 5 μm). In the case of depth, it increased from 110 ± 30 nm (G-0/1) to values close to 400 nm (G-0/5 and G-0/10).

Interestingly, the addition of magnesium particles changed the appearance of the films with surfactant (Fig. 7). In the case of G-3/0 a completely flat surface was observed, similar to G-0/0, with no remarkable singularities, and with a roughness very close to G-0/0 (Sa = 7 ± 2 nm). When the surfactant was added, magnesium particles caused the structures to become very regular and well distributed, and the size was slightly higher for G-3/10 (Fig. 8, width 1.8 ± 0.6 μm and depth 340 ± 140 nm) than for G-3/1 and G-3/5. Again, note that magnesium helped to disperse the surfactant in the PLA matrix.

3.2.2. Topography of degraded films

Films cast on glass degrade differently from those cast on silicone, especially in the case of absence of surfactant: looking at Fig. 8, holes appeared after 28 days in the sample without magnesium, and if magnesium was present, holes had already appeared at 7 days (no such degradation was observed with silicone). Some representative images are given in Fig. 9.

In addition to topography, hydrophobicity of the film is affected by the surface on which it is deposited. A previous work of our group showed that films deposited on silicone and glass have different values of hydrophobicity [23], the films deposited on glass being hydrophilic, while those deposited on silicone are hydrophobic, with the hydrophilicity-hydrophobicity threshold set at 90° [50]. The films of this study were also characterized by goniometry and the water contact angles obtained were 107° ± 1°; 99° ± 5°; 75° ± 5° and 67° ± 5° for S-0/0; S-3/0; G-0/0 and G-3/0, respectively. The hydrophilicity of films on

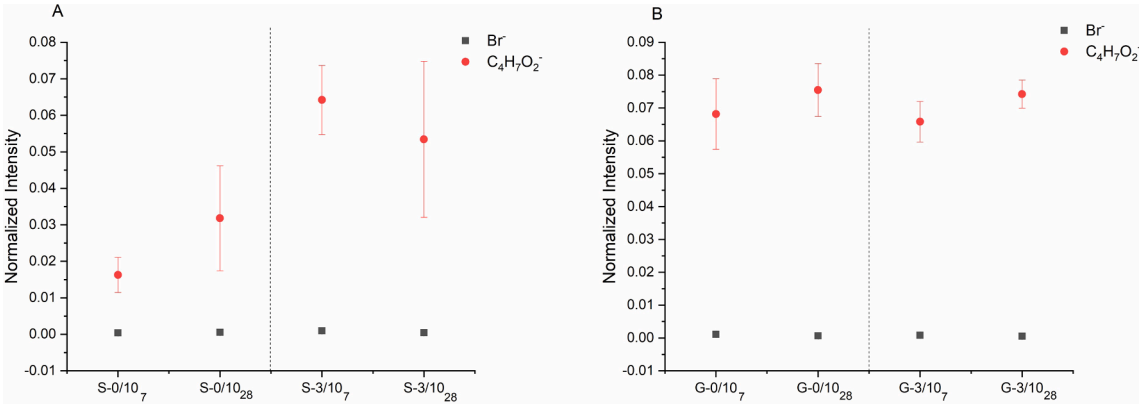

Fig. 6. Chemical surface analysis of the films provided by ToF-SIMS surface mass spectra. Br^- is taken as a representative fragment of the CTAB and $C_4H_7O_2^-$ is taken as representative of PLA.

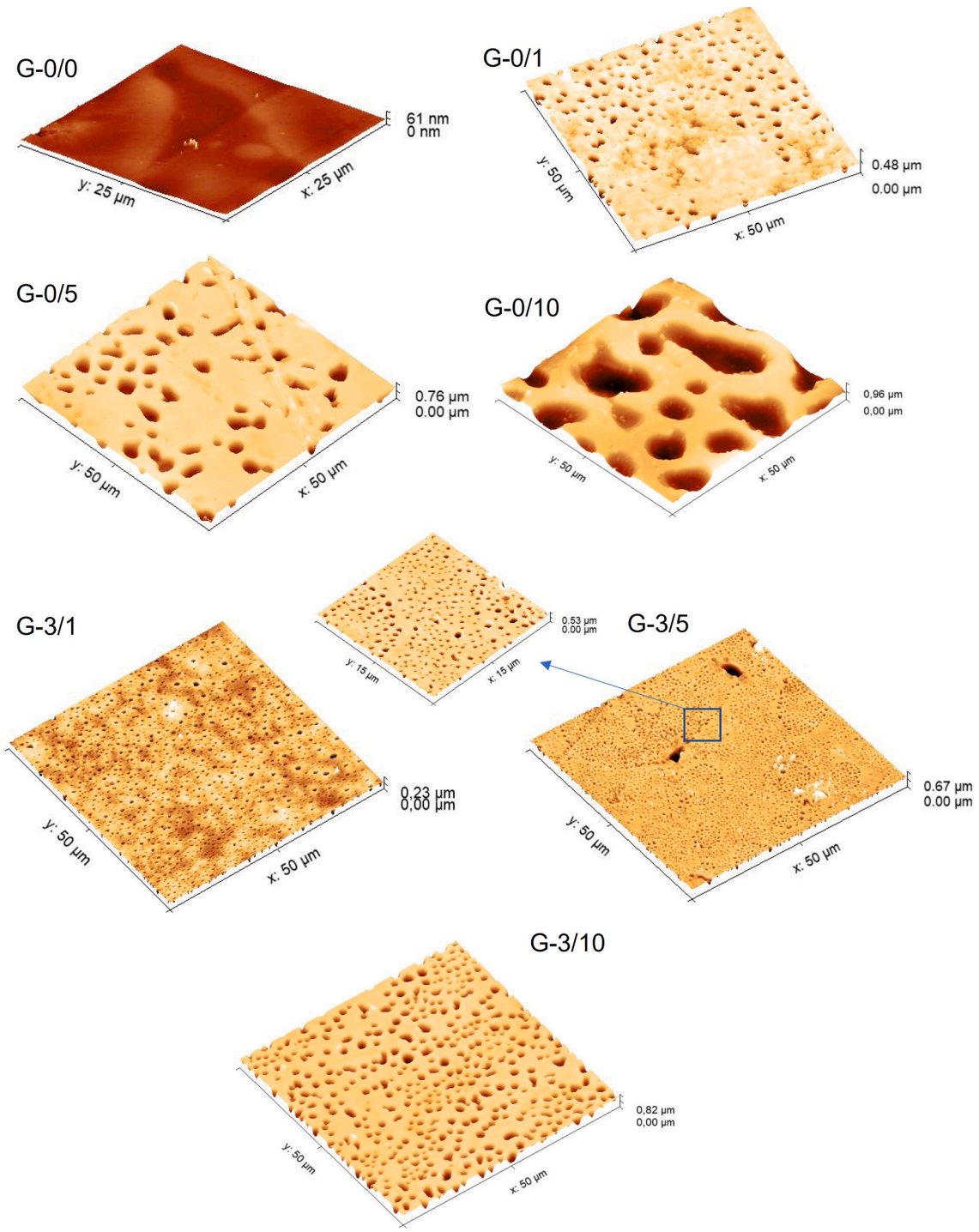

Fig. 7. Representative images of the films deposited on glass without and with magnesium and with different concentrations of CTAB. All the images are topographical.

glass facilitates the degradation of the polymer in an aqueous environment such as PBS, with small holes appearing on the polymer favouring its release into the environment.

Degradation of films with surfactant must be associated with two contributions: on the one hand, release of the surfactant, and on the other hand, release of the polymer. This means that for films without magnesium, the density of the holes increases and they become more irregular and increase in size (compare Figs. 7 and 9); in the case of G-0/10_{28} the smaller holes are not visible (also Fig. 8).

In the case of magnesium-containing films, degradation also causes the circular geometry of the holes to become more irregular, with the formation of bonds between nearby holes, which, in the case of G-3/10_{28}, leads to the appearance of a labyrinth-like surface lattice.

Compositional analysis of the outermost surface layer of the films after degradation (Fig. 6) shows that the films surface released all surface surfactant content after 7 days of degradation. It should be noted that the hydrophilicity of glass causes a small amount of the polymer/surfactant mixture to spill over the edges of the support when preparing the samples. This unavoidable artifact causes estimation of surfactant content in the solution to be affected with considerable uncertainty.

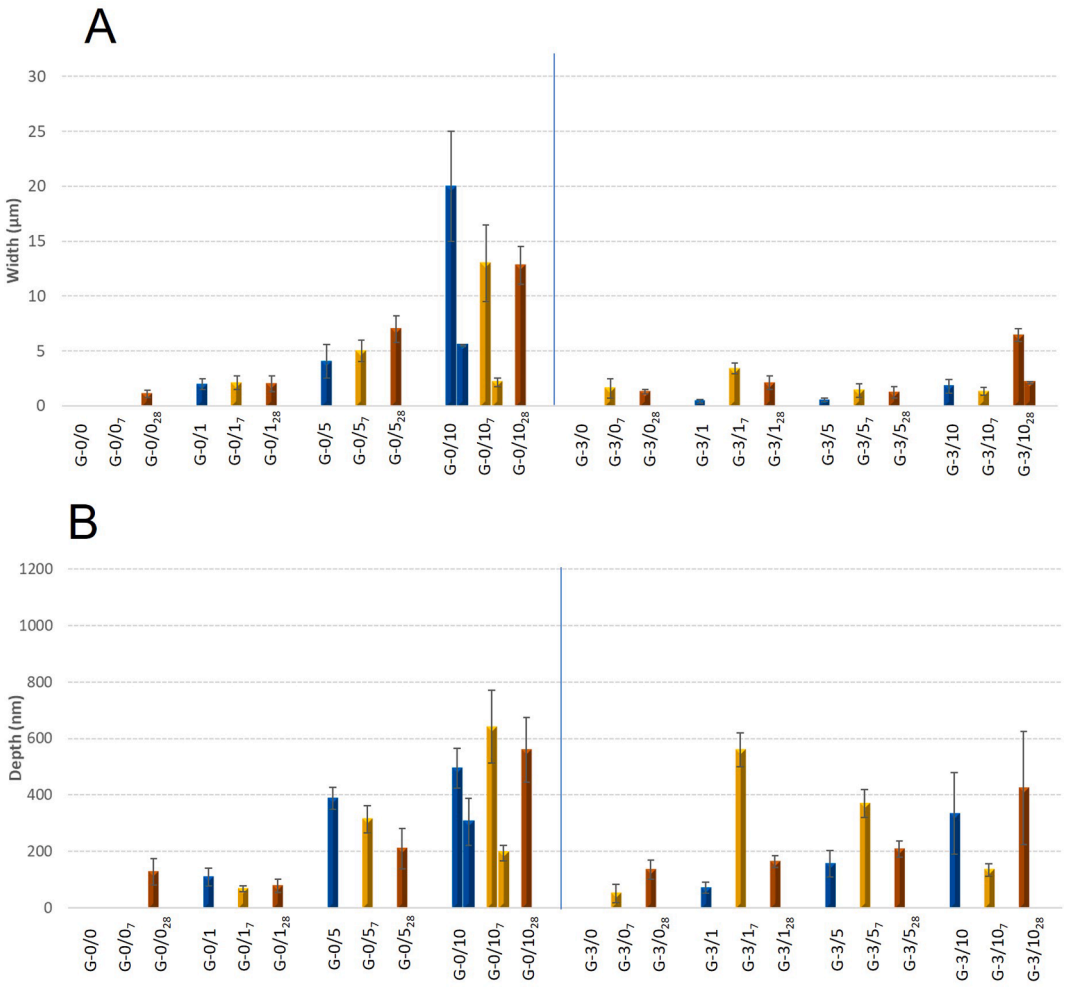

Fig. 8. Quantification of the features (holes) observed on films deposited on glass through their width (A) and depth (B). Two bars for the same sample indicate the presence of two completely different hole populations.

The formation of structures as well as their shape is associated with the three variables we have studied: surfactant concentration, presence of magnesium and type of support used in the preparation of the films. Table 1 summarizes the effect of each of the variables used on shape and size of the structures. It can be seen that structures on silicone are more stable than on glass. The degradation process modifies them less; only the magnesium causes, in the case of higher CTAB, these structures to deform over time, doubling their size. The high hydrophobicity of the silicone probably favours hydrophobic interactions between the surface and the PLA polymeric chains, forming a more compact matrix that is less susceptible to alteration in aqueous environments, as is the case with PBS. This idea is also supported by the fact that the surface of films deposited on silicone is hydrophobic, as opposed to glass, which is hydrophilic.

The surfactant exclusion zones on the surfaces of films deposited on glass are large and irregular, reaching dimensions of 20 μm in width. Nevertheless, interestingly, magnesium was able to distribute this surfactant very uniformly on the matrix and, in this case, highly regular exclusion zones of no more than 2 μm were observed. In general, the hydrophilic character of the films on glass leads to degradation of the structures formed with immersion time in PBS.

Among the various applications of the structures presented in this work are the design of antimicrobial surfaces as well as the development of surfaces that enhance cell adhesion. The size of the structures would determine one utility or another and, in the case of antibacterial topographies, it is usually worked with sizes below (or of the order) of the dimensions of the bacteria [30,40], so films deposited on glass with low concentrations of CTAB and with magnesium as a dispersant can be a good option. Some authors have even shown reductions in the order of 30–45% in adhesion of different bacterial strains to surfaces with hole-like structures with widths of 3 μm to 6 μm [36] and films on silicone can also develop anti-adhesive behaviour, with temporary stability. In the case of cell adhesion, beneficial topographies can include patterns up to several microns in size. Certain applications require porous materials that can reproduce biological architectures such as that which exists in highly porous bone matrices. Porous interfaces can increase the biomechanical interlocking between implant and the native bone tissue, upregulating implant fixation. In a very recent paper by R. Akoumeh et al. authors prepared microporous surfaces from immiscible polymers and observed, working with porosity ranges from approximately 7 μm to 37 μm, that cell adhesion on microporous surfaces was enhanced, evidencing the role of surface topography in cell adhesion [27]. We would also like to point out that, although we have quantified the changes in the micro-topographies with degradation, it is very likely that an *in vivo* environment will modify these patterns, especially considering that the adhesion of cells and/or bacteria to the surface can enhance or slow down the process of CTAB release to the medium as well as alter the deposition of salts from the degradation medium.

The different surface finishes observed for PLA-magnesium/CTAB provide a wide spectrum of topographies with micro-structures or micropores of different sizes that can be very useful in the biomedical field. The advantage of this study over others is the versatility in terms of

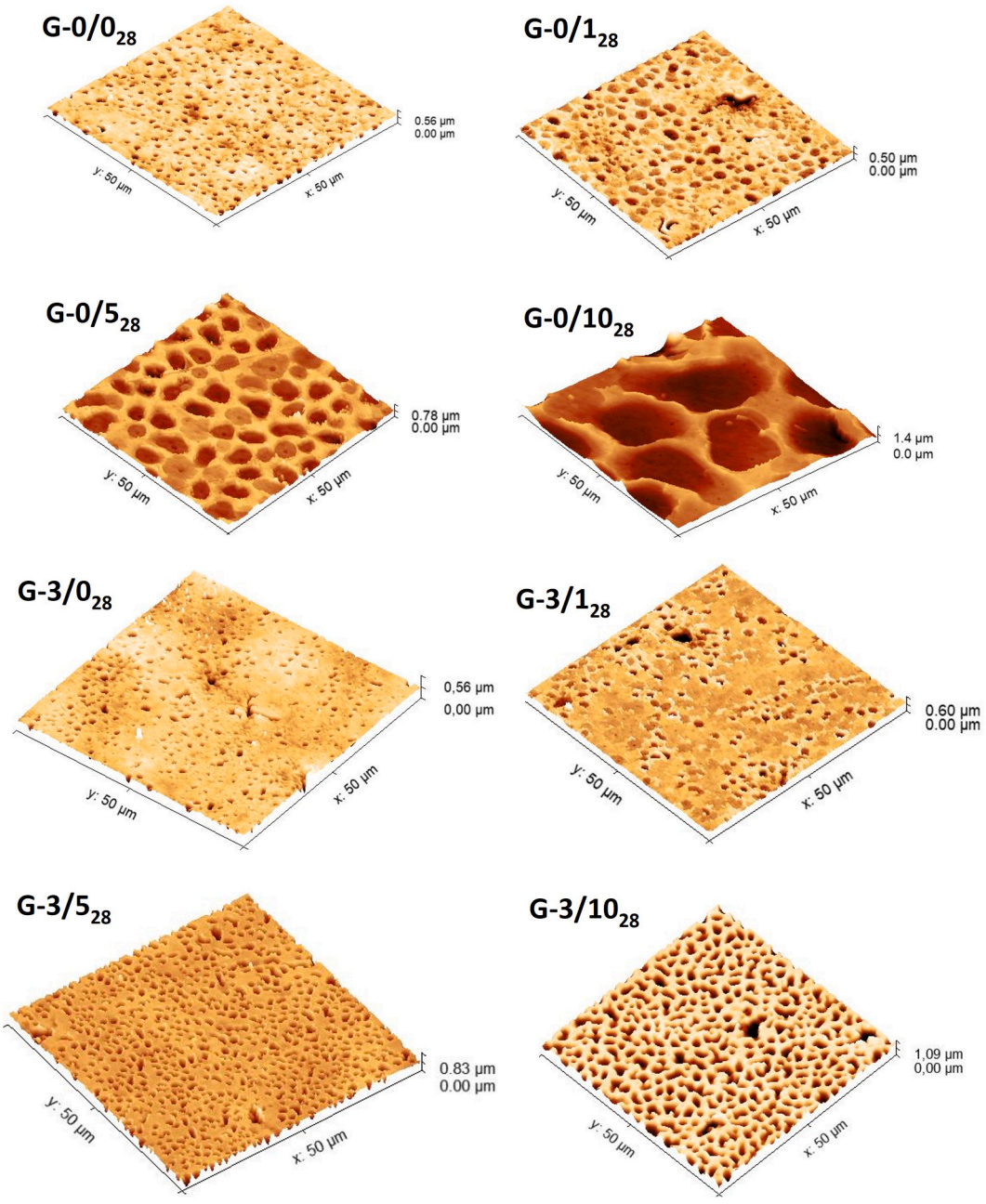

Fig. 9. AFM topographical images of degraded films cast on glass, without and with magnesium and with different concentrations of CTAB.

fabrication: film production can be made on a massive scale and very cost-effectively, without the need for equipment based on lithography, laser etching, molecular self-assembly, plasma spraying or ion implantation [40,42].

4. Conclusions

It is possible to generate micro-structured surfaces with hole-like patterns of different sizes on PLA films by adding different concentrations of surfactant to the polymer matrix, using magnesium as a dispersant, and using different support-substrates.

The diversity of conditions allows hole sizes from sub-micrometer scale to several microns in width to be obtained, these patterns being more stable when silicone is used as a solvent-casting support. The bio-applications are therefore wide-ranging, from the generation of anti-microbial surfaces to surfaces that promote cell integration.

The film production method can be done on a massive scale and it is economically very attractive, since it does not need any equipment based on lithography, laser etching, molecular self-assembly, plasma spraying or ion implantation, which are currently being used with polymers to generate structured surfaces.

CRediT authorship contribution statement

Amparo M. Gallardo-Moreno: Conceptualization, Data curation, Formal analysis, Funding acquisition, Investigation, Methodology, Supervision, Writing – original draft, Writing – review & editing. **Verónica Luque-Agudo:** Data curation, Formal analysis, Investigation, Writing – original draft. **M. Luisa González-Martín:** Conceptualization, Funding acquisition, Investigation, Methodology, Supervision, Writing – review & editing. **Margarita Hierro-Oliva:** Data curation, Formal analysis, Investigation, Supervision, Writing – original draft.

Table 1
Summary of the effect of magnesium, CTAB, substrate and degradation time on the size of the micro-structures found. Size quantification in this table is approximate, exact values are in Figs. 2 and 8.

Silicone		
CTAB (1%, 5%, 10%)		YES: circular-like structures (between 1 and 5 μm) Size increases with CTAB concentration
Magnesium		NO
Degradation (without Mg)	7 days	NO: deformation of structures
	28 days	NO: deformation of structures
Degradation (with Mg)	7 days	SOME: deformation with S-3/10_7
	28 days	SOME: deformation with S-3/10_{28}
Glass		
CTAB (1%, 5%, 10%)		YES: irregular and large structures (between 2 and 20 μm) Size increases with CTAB concentration
Magnesium		YES: Mg makes regular and small structures (between 0.5 and 2 μm)
Degradation (without Mg)	7 days	NO: deformation of structures
	28 days	YES: deformation of structures in all cases
Degradation (with Mg)	7 days	YES: deformation of structures in all cases
	28 days	YES: deformation of structures in all cases

Declaration of Competing Interest

The authors declare that they have no known competing financial interests or personal relationships that could have appeared to influence the work reported in this paper.

Acknowledgements

Authors are grateful to Junta de Extremadura and FEDER for grant numbers GR21119 and IB20092. Thanks also to project RTI2018-096862-B-I00, supported by MCIN/ AEI /10.13039/501100011033/ FEDER "Una manera de hacer Europa". ToF-SIMS, contact angle and surface tension measurements were performed by the ICTS "NANBIOSIS", more specifically by the Surface Characterization and Calorimetry Unit of the CIBER in Bioingeniería, Biomateriales y Nanomedicina (CIBER-BBN) and the SACSS-SAIUEx of the Universidad de Extremadura (UEx). Special appreciation to James Mc-Cue for assistance in language editing.

Appendix A. Supplementary material

Supplementary data to this article can be found online at https://doi.org/10.1016/j.apsusc.2022.153676.

References

[1] A. Ashothaman, J. Sudha, N. Senthilkumar, Materials Today : Proceedings A comprehensive review on biodegradable polylactic acid polymer matrix composite material reinforced with synthetic and natural fibers, Mater. Today:. Proc. (2021), https://doi.org/10.1016/j.matpr.2021.07.047.
[2] M. Murariu, P. Dubois, PLA composites : From production to properties, Adv. Drug Deliv. Rev. 107 (2016) 17–46, https://doi.org/10.1016/j.addr.2016.04.003.
[3] A.J.R. Lasprilla, G.A.R. Martinez, B.H. Lunelli, A.L. Jardini, R. Maciel, Poly-lactic acid synthesis for application in biomedical devices — A review, Biotechnol. Adv. 30 (2012) 321–328, https://doi.org/10.1016/j.biotechadv.2011.06.019.
[4] Y. Byun, S. Whiteside, R. Thomas, M. Dharman, J. Hughes, Y.T. Kim, The effect of solvent mixture on the properties of solvent cast polylactic acid (PLA) film, J. Appl. Polym. Sci. 124 (2012) 3577–3582, https://doi.org/10.1002/app.34071.
[5] S. Sato, T. Wada, R. Ido, Y. Murakoshi, S. Kanehashi, K. Nagai, Dependence of alcohol vapor-induced crystallization on gas and vapor permeabilities of poly (lactic acid) films, J. Appl. Polym. Sci. 131 (2014) 1–9, https://doi.org/10.1002/app.40140.
[6] Y. Chen, L.M. Geever, C.L. Higginbotham, D.M. Devine, Analysis of the mechanical properties of solvent cast blends of PLA/PCL, Appl. Mech. Mater. 679 (2014) 50–56, https://doi.org/10.4028/www.scientific.net/AMM.679.50.
[7] V. Luque-Agudo, D. Romero-Guzmán, M. Fernández-Grajera, M.L. González-Martín, A.M. Gallardo-Moreno, Aging of Solvent-Casting PLA-Mg Hydrophobic Films: Impact on Bacterial Adhesion and Viability, Coatings 9 (2019) 814, https://doi.org/10.3390/coatings9120814.
[8] P. Takkalkar, M.J. Tobin, J. Vongsvivut, T. Mukherjee, S. Nizamuddin, G. Griffin, N. Kao, Structural, thermal, rheological and optical properties of poly(lactic acid) films prepared through solvent casting and melt processing techniques, J. Taiwan Inst. Chem. Eng. 104 (2019) 293–300.
[9] T. Paragkumar N, D. Edith, J.-L. Six, Surface characteristics of PLA and PLGA films, Appl. Surf. Sci. 253 (5) (2006) 2758–2764.
[10] T. Fukuoka, T. Morita, A. Saika, H. Habe, Application of glycolipid biosurfactants as surface modifiers in bioplastics, J. Oleo Sci. 67 (2018) 1609–1616, https://doi.org/10.5650/jos.ess18116.
[11] V. Luque-Agudo, A.M. Gallardo-Moreno, M.L. González-Martín, Influence of Solvent and Substrate on Hydrophobicity of PLA Films, Polymers (Basel) 13 (2021) 4289, https://doi.org/10.3390/polym13244289.
[12] S.A. Cruz, L.A. Onoue, C.M. Paranhos, E. Longo, Effect of sepiolite on the quiescent and non-quiescent crystallization behaviour of the biodegradable poly(Lactic acid) prepared via casting and melting, Express, Polym. Lett. 13 (2019) 825–834, https://doi.org/10.3144/expresspolymlett.2019.71.
[13] C.G. Silva, P.A.L. Campini, D.B. Rocha, D.S. Rosa, The influence of treated eucalyptus microfibers on the properties of PLA biocomposites, Compos. Sci. Technol. 179 (2019) 54–62, https://doi.org/10.1016/j.compscitech.2019.04.010.
[14] M. Safaei, R. Roosta Azad, Preparation and characterization of poly-lactic acid based films containing propolis ethanolic extract to be used in dry meat sausage packaging, J. Food Sci. Technol. 57 (2020) 1242–1250, https://doi.org/10.1007/s13197-019-04156-z.
[15] A. Jaya, B. Kunhanna, K. Ramachandra, B. Shivarama, A. Glorious, Spectral, morphological and optical studies on bischalcone doped polylactic acid (PLA) thin fi lms as luminescent and UV radiation blocking materials, Opt. Mater. (Amst). 90 (2019) 145–151, https://doi.org/10.1016/j.optmat.2019.02.028.
[16] F. Alam, V.R. Shukla, K.M. Varadarajan, S. Kumar, Microarchitected 3D printed polylactic acid (PLA) nanocomposite scaffolds for biomedical applications, J. Mech. Behav. Biomed. Mater. 103 (2020) 103576.
[17] J. Ahmed, Y.A. Arfat, E. Castro-Aguirre, R. Auras, Thermal properties of ZnO and bimetallic Ag–Cu alloy reinforced poly(lactic acid) nanocomposite films, J. Therm. Anal. Calorim. 125 (2016) 205–214, https://doi.org/10.1007/s10973-016-5402-1.
[18] W. Mustafa, U. Azhar, S. Tabassum, M. Jamal, S.A. Siddiqi, M. Tariq, N. Muhammad, A. Asif, A.A. Chaudhry, F. Sharif, Doping and Incorporation of Hydroxyapatite in Development of PU-PLA Electrospun Osteogenic Membranes, J. Polym. Environ. 28 (2020) 2988–3002, https://doi.org/10.1007/s10924-020-01764-1.
[19] A. Ferrández-Montero, M. Lieblich, R. Benavente, J.L. González-Carrasco, B. Ferrari, Study of the matrix-filler interface in PLA/Mg composites manufactured by Material Extrusion using a colloidal feedstock, Addit. Manuf. 33 (2020) 101142, https://doi.org/10.1016/j.addma.2020.101142.
[20] A. Ferrandez-Montero, M. Lieblich, R. Benavente, J.L. González-Carrasco, B. Ferrari, New approach to improve polymer-Mg interface in biodegradable PLA/Mg composites through particle surface modification, Surf. Coat. Technol. 383 (2020) 125285, https://doi.org/10.1016/j.surfcoat.2019.125285.
[21] J. Zhang, S.J. Severtson, C.J. Houtman, Characterizing the distribution of sodium alkyl sulfate surfactant homologues in water-based, acrylic pressure-sensitive adhesive films, J. Phys. Chem. B 115 (25) (2011) 8138–8144.
[22] I.C. Gîfu, M.E. Maxim, L.O. Cinteza, M. Popa, L. Aricov, A.R. Leontieș, M. Anastasescu, D.-F. Anghel, R. Ianchis, C.M. Ninciuleanu, S.G. Burlacu, C. L. Nistor, C. Petcu, Antimicrobial activities of hydrophobically modified poly (acrylate) films and their complexes with different chain length cationic surfactants, Coatings 9 (4) (2019) 244.
[23] M. Hierro-Oliva, V. Luque-Agudo, A.M. Gallardo-Moreno, M.L. González-Martín, Characterization of Magnesium-Polylactic Acid Films Casted on Different Substrates and Doped with Diverse Amounts of CTAB, Molecules 26 (2021) 4811, https://doi.org/10.3390/molecules26164811.
[24] M.C. Fernández-calderón, D. Romero-guzmán, A. Ferrández-montero, C. Pérez-giraldo, J.L. González-carrasco, M. Lieblich, R. Benavente, B. Ferrari, M. L. González-martín, A.M. Gallardo-moreno, Colloids and Surfaces B : Biointerfaces Impact of PLA / Mg fi lms degradation on surface physical properties and bio fi lm survival, Colloids Surf., B 185 (2020) 110617, https://doi.org/10.1016/j.colsurfb.2019.110617.
[25] M.C. Fernández-Calderón, S.C. Cifuentes, M.A. Pacha-Olivenza, A.M. Gallardo-Moreno, L. Saldaña, J.L. González-Carrasco, M.T. Blanco, N. Vilaboa, M. L. González-Martín, C. Pérez-Giraldo, Antibacterial effect of novel biodegradable and bioresorbable PLDA/Mg composites, Biomed. Mater. 12 (2017) 015025, https://doi.org/10.1088/1748-605X/aa5a14.
[26] S.C. Cifuentes, F. Bensiamar, A.M. Gallardo-Moreno, T.A. Osswald, J.L. González-Carrasco, R. Benavente, M.L. González-Martín, E. García-Rey, N. Vilaboa, L. Saldaña, Incorporation of Mg particles into PDLLA regulates mesenchymal stem cell and macrophage responses, J. Biomed. Mater. Res. Part A 104 (4) (2016) 866–878.
[27] R. Akoumeh, T. Elzein, E. Martínez-campos, F. Reviriego, J. Rodríguez-hern, Fabrication of porous films from immiscible polymer blends: Role of the surface structure on the cell adhesion, Polym. Test. 91 (2020), https://doi.org/10.1016/j.polymertesting.2020.106797.
[28] P. Sangnak, P. Seananud, P. Daniel, P. Ruamcharoen, C. Wayakron, I. Mol, Antimicrobial film from PLA / NR-grafted-modified chitosan-chelated-silver ions blend, React. Funct. Polym. 169 (2021) 105073, https://doi.org/10.1016/j.reactfunctpolym.2021.105073.

[29] S. Shankar, J. Rhim, International Journal of Biological Macromolecules Preparation of antibacterial poly (lactide)/poly (butylene adipate- co - terephthalate) composite films incorporated with grapefruit seed extract, Int. J. Biol. Macromol. 120 (2018) 846–852, https://doi.org/10.1016/j.ijbiomac.2018.09.004.
[30] S. Won, K.S. Phillips, H. Gu, M. Kazemzadeh-narbat, Biomaterials How microbes read the map: Effects of implant topography on bacterial adhesion and biofilm formation, Biomaterials 268 (2021) 120595, https://doi.org/10.1016/j.biomaterials.2020.120595.
[31] A. Francone, S. Merino, A. Retolaza, J. Ramiro, S.A. Alves, J.V. de Castro, N. M. Neves, A. Arana, J.M. Marimon, C.M.S. Torres, N. Kehagias, Impact of surface topography on the bacterial attachment to micro- and nano-patterned polymer films, Surf. Interfaces 27 (2021) 101494.
[32] S. Wu, B. Zhang, Y. Liu, X. Suo, H. Li, Influence of surface topography on bacterial adhesion: A review (Review), Biointerphases 060801 (2018), https://doi.org/10.1116/1.5054057.
[33] S. Coppari, S. Ramakrishna, L. Teodori, M.C. Albertini, ScienceDirect Cell signalling and biomaterials have a symbiotic relationship as demonstrated by a bioinformatics study: The role of surface topography, 2021.
[34] S. Zangi, I. Hejazi, J. Sey, E. Hejazi, H. Ali, S. Mohammad, Tuning cell adhesion on polymeric and nanocomposite surfaces: Role of topography versus superhydrophobicity, Mater. Sci. Eng.: C 63 (2016) 609–615.
[35] N. Lu, W. Zhang, Y. Weng, X. Chen, Y. Cheng, P. Zhou, Fabrication of PDMS surfaces with micro patterns and the effect of pattern sizes on bacteria adhesion, Food Control 68 (2016) 344–351, https://doi.org/10.1016/j.foodcont.2016.04.014.
[36] D. Perera-Costa, J.M. Bruque, M.L. González-Martín, A.C. Gómez-García, V. Vadillo-Rodríguez, Studying the Influence of Surface Topography on Bacterial Adhesion using Spatially Organized Microtopographic Surface Patterns, Langmuir 30 (16) (2014) 4633–4641.
[37] X. Ge, Y. Leng, X. Lu, F. Ren, K. Wang, Y. Ding, M. Yang, Bacterial responses to periodic micropillar array, J. Biomed. Mater. Res. Part A 103 (1) (2015) 384–396.
[38] A. Allion, J.-P. Baron, L. Boulange-Petermann, Impact of surface energy and roughness on cell distribution and viability, Biofouling. 22 (2006) 269–278, https://doi.org/10.1080/08927010600902789.
[39] A.-K. Meinshausen, M. Herbster, C. Zwahr, M. Soldera, A. Müller, T. Halle, A. F. Lasagni, J. Bertrand, Aspect ratio of nano/microstructures determines Staphylococcus aureus adhesion on PET and titanium surfaces, J. Appl. Microbiol. 131 (3) (2021) 1498–1514.
[40] A. Tripathy, P. Sen, B.o. Su, W.H. Briscoe, Natural and bioinspired nanostructured bactericidal surfaces, Adv. Colloid Interface Sci. 248 (2017) 85–104.
[41] J. Szewczenko, J. Marciniak, W. Kajzer, A. Kajzer, Metallic biomaterials, titanium alloys, corrosion resistance, mechanical processing, anodic oxidation, Arch. Metall. Mater. 61 (2016) 695–700, https://doi.org/10.1515/amm-2016-0118.
[42] M. Jurak, A.E. Wiącek, A. Ładniak, K. Przykaza, K. Szafran, What affects the biocompatibility of polymers? Adv. Colloid Interface Sci. 294 (2021) 102451, https://doi.org/10.1016/j.cis.2021.102451.
[43] Y. Li, J. Yan, W. Zhou, P. Xiong, P. Wang, W. Yuan, Y. Zheng, Y. Cheng, Bioactive Materials In vitro degradation and biocompatibility evaluation of typical biodegradable metals (Mg/Zn/Fe) for the application of tracheobronchial stenosis, Bioact. Mater. 4 (2020) 114–119, https://doi.org/10.1016/j.bioactmat.2019.01.001.
[44] A. Ferrández-Montero, M. Lieblich, J.L. González-Carrasco, R. Benavente, V. Lorenzo, R. Detsch, A.R. Boccaccini, B. Ferrari, Development of biocompatible and fully bioabsorbable PLA/Mg films for tissue regeneration applications, Acta Biomater. 98 (2019) 114–124, https://doi.org/10.1016/j.actbio.2019.05.026.
[45] X. Xu, Y.e. Liu, Z. Guo, X.-Z. Song, X. Qi, Z. Dai, Z. Tan, Synthesis of surfactant-modified ZIF-8 with controllable microstructures and their drug loading and sustained release behaviour, IET Nanobiotechnol. 14 (7) (2020) 595–601.
[46] V. Luque-Agudo, M.C. Fernández-Calderón, M.A. Pacha-Olivenza, C. Pérez-Giraldo, A.M. Gallardo-Moreno, M.L. González-Martín, The role of magnesium in biomaterials related infections, Colloids Surf., B 191 (2020) 110996, https://doi.org/10.1016/j.colsurfb.2020.110996.
[47] A. du Chesne, B. Gerharz, G. Lieser, The segregation of surfactant upon film formation of latex dispersions: An investigation by energy filtering transmission electron microscopy, Polym. Int. 43 (1997) 187–196, https://doi.org/10.1002/(sici)1097-0126(199706)43:2<187::aid-pi752>3.3.co;2-8.
[48] J. Mallégol, J.P. Gorce, O. Dupont, C. Jeynes, P.J. McDonald, J.L. Keddie, Origins and effects of a surfactant excess near the surface of waterborne acrylic pressure-sensitive adhesives, Langmuir 18 (2002) 4478–4487, https://doi.org/10.1021/la0117698.
[49] M.J. Monteiro, M. Sjöberg, J. van der Vlist, C.M. Göttgens, Synthesis of butyl acrylate-styrene block copolymers in emulsion by reversible addition-fragmentation chain transfer: Effect of surfactant migration upon film formation, J. Polym. Sci., Part A: Polym. Chem. 38 (2000) 4206–4217, https://doi.org/10.1002/1099-0518(20001201)38:23<4206::AID-POLA60>3.0.CO;2-E.
[50] S. Latthe, C. Terashima, K. Nakata, A. Fujishima, Superhydrophobic Surfaces Developed by Mimicking Hierarchical Surface Morphology of Lotus Leaf, Molecules 19 (2014) 4256–4283, https://doi.org/10.3390/molecules19044256.